BIOCHEMISTRY
including biophysical chemistry & molecular biology

Article

pubs.acs.org/biochemistry

Expression, Purification, and Reconstitution of the Voltage-Sensing Domain from Ci-VSP

Qufei Li, Vishwanath Jogini,[†] Sherry Wanderling, D. Marien Cortes,[‡] and Eduardo Perozo*

Department of Biochemistry and Molecular Biology, Center for Integrative Science, University of Chicago, Chicago, Illinois 60637, United States

ABSTRACT: The voltage-sensing domain (VSD) is the common scaffold responsible for the functional behavior of voltage-gated ion channels, voltage sensitive enzymes, and proton channels. Because of the position of the voltage dependence of the available VSD structures, at present, they all represent the activated state of the sensor. Yet in the absence of a consensus resting state structure, the mechanistic details of voltage sensing remain controversial. The voltage dependence of the VSD from Ci-VSP (Ci-VSD) is dramatically right shifted, so that at 0 mV it presumably populates the putative resting state. Appropriate biochemical methods are an essential prerequisite for generating sufficient amounts of Ci-VSD protein for high-resolution structural studies. Here, we present a simple and robust protocol for the expression of eukaryotic Ci-VSD in *Escherichia coli* at milligram levels. The protein is pure, homogeneous, monodisperse, and well-folded after solubilization in Anzergent 3-14 at the analyzed concentration (~0.3 mg/mL). Ci-VSD can be reconstituted into liposomes of various compositions, and initial site-directed spin labeling and electron paramagnetic resonance (EPR) spectroscopic measurements indicate its first transmembrane segment folds into an α-helix, in agreement with the homologous region of other VSDs. On the basis of our results and enhanced relaxation EPR spectroscopy measurement, Ci-VSD reconstitutes essentially randomly in proteoliposomes, precluding straightforward application of transmembrane voltages in combination with spectroscopic methods. Nevertheless, these results represent an initial step that makes the resting state of a VSD accessible to a variety of biophysical and structural approaches, including X-ray crystallography, spectroscopic methods, and electrophysiology in lipid bilayers.

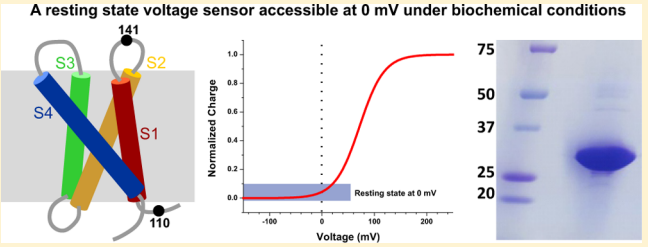

In most members of the voltage-gated cationic channel superfamily, the voltage-sensing domain (VSD) is responsible for the electromechanical transduction that couples transmembrane protein motion to an increase in membrane permeability.[1,2] The identification of the *Ciona intestinalis* voltage-dependent phosphatase (Ci-VSP),[3] for which the activity of a membrane-bound enzyme is directly modulated by transmembrane voltage via coupling with a bona fide VSD (Ci-VSD), suggests that VSDs can operate as independent functional domains. Furthermore, VSDs have been also proven to be the key structural scaffold for proton channels.[4,5] In all known VSDs, both the architecture and voltage sensing mechanism are conserved.[6]

The conserved VSD scaffold is formed by four transmembrane segments (S1−S4), arranged in an antiparallel four-helix bundle. Positively charged residues (R/K) on fourth transmembrane segment S4[7] reorient in response to changes in voltage across the membrane, leading to subsequent physiological responses. This conformational change produces a transient charge movement that generates a nonlinear capacitive current described in the early 1970s as the gating current,[8] and represents the electrical expression of the structural rearrangements in all VSDs.[9] Our knowledge of the functional properties of VSD comes predominantly from the gating current measurements in Shaker,[10,11] a eukaryotic potassium channel from *Drosophila*.[12] Long-term efforts to structurally characterize Shaker have been limited by the lack of a robust biochemical prep, and at the same time, VSDs with available high-resolution structures have had limited or no gating current data. The fact that Ci-VSD gating current measurements can be readily obtained[3,13] makes this system an attractive candidate for correlating functional and structural information in the same VSD system. Clearly, this would help sort out the potential differences between VSD homologues and create a reference point for reinterpreting the available information in the field.

Ultimately, determining the mechanism of voltage sensing will require high-resolution structures of VSDs in at least two functionally relevant states. First, the activated ("Up") conformation is found when the transmembrane field intensity is eliminated or reverses its polarity. This conformation is best represented by the available VSD structures KvAP,[14,15] Kv1.2 chimera,[16] NavAb,[17] and NavRh,[18] all determined at 0 mV. Second, the elusive resting ("Down") conformation, in which charges are directly under the influence of the transmembrane electric field, is still experimentally unavailable. At a minimum, determining the structure of an alternative state (other than the Up state) would go a long way toward clarifying a great deal of

Received: July 21, 2012
Revised: September 17, 2012
Published: September 18, 2012

dx.doi.org/10.1021/bi300980q | *Biochemistry* 2012, 51, 8132−8142

the existing controversies. The voltage dependence of Ci-VSD is significantly right-shifted (Figure 1A), a fact that would make the Down state VSD accessible to experimental manipulations in the absence of an asymmetric voltage.

Ci-VSD is an interesting model not only with regard to the voltage sensing mechanism but also as a structural stand-in for proton channel Hv1. A point mutation in the VSD of Shaker is able to generate a hyperpolarization-driven ion current (the omega current[19]) that allows proton permeation under some conditions.[20] On the basis of sequence and functional correlations, it has been suggested that Ci-VSD might represent an evolutionary intermediate between the voltage sensor in voltage-gated ion channels and proton channels.[21] Though Ci-VSD functions as a voltage sensor, its sequence is closer to that of proton channels than to all four of the VSDs with available high-resolution structures. Thus, structural studies on the resting state VSD of Ci-VSD could not only yield valuable information about the basic principles of a voltage sensing mechanism but also provide a better homology model for the proton channel, for which there are no high-resolution structures so far.

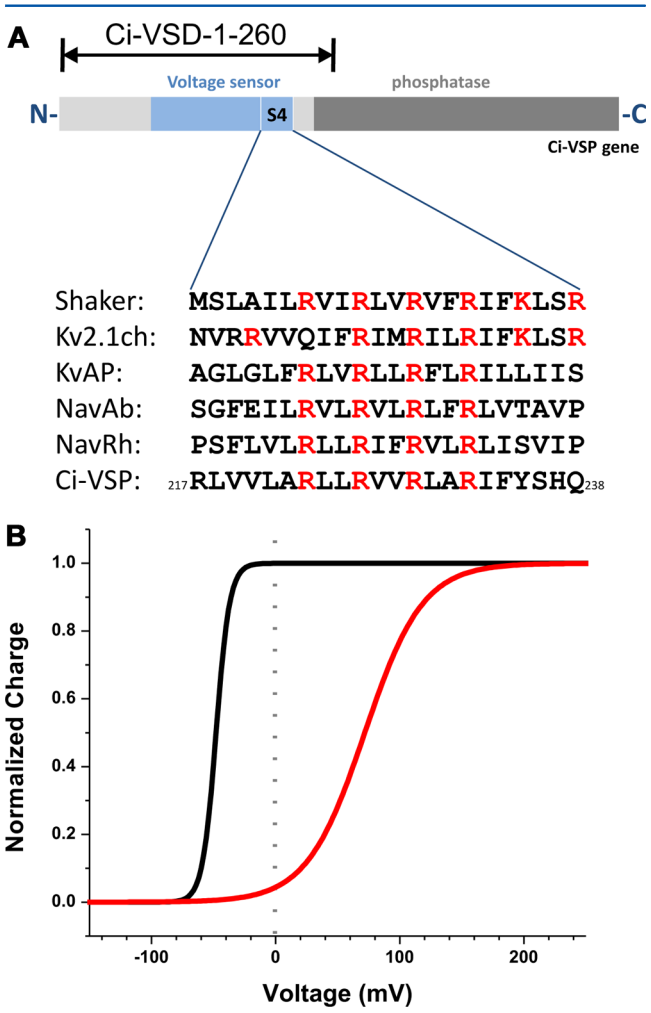

Figure 1. Sequence alignment and function comparison of Ci-VSD with existing VSDs. (A) The gene of Ci-VSP consists of the N-terminus, the voltage-sensing domain, a linker, and the phosphatase domain. The first 260 residues, indicated by the arrow at the top, is our current interest for biochemical preparation. The sequence of the fourth transmembrane segment (S4) of Ci-VSP was aligned with homologous sequences from voltage-gated ion channels. The positively charged residues (R/K) were distributed at every third position and are primarily responsible for voltage sensing and highly conserved. (B) Relationship between the charge movement and the test pulse amplitude (Q–V curve) of VSDs from a typical potassium channel Shaker (black) and Ci-VSP (red). The curves was simulated with a $V_{1/2}$ of −48 mV and a z of 4.7 for Shaker[38] and a $V_{1/2}$ of 71.8 mV and a z of 1.1 for Ci-VSP.[3] The dotted line at 0 mV indicates the potential states of VSDs under biochemical conditions in the absence of asymmetric voltage across the proteins: Shaker's VSD in the activated state (or Up state) and Ci-VSD in the resting state (or Down state).

Encouraged by the potential of Ci-VSD as a pathway for answering key questions regarding voltage sensing in cationic and proton channels, we have developed a biochemical approach to generating milligram-scale preparations of homogeneous Ci-VSD for potential biophysical studies. Initial characterization of solubilized preparations suggests that Ci-VSD is stable in five detergents at a high concentration (20 mg/mL) for at least a week. Ci-VSD can be reconstituted into liposomes of various compositions and is monodisperse in POPC/POPG liposomes in the long term, a fact that provides suitable conditions for EPR, solid state NMR, and electrophysiologcal approaches. This methodology shall play a key role in our attempts to understand the molecular basis of voltage-dependent gating in a variety of biological systems.

EXPERIMENTAL PROCEDURES

Materials. cDNA of Ci-VSP-1−576 in the Sp6 vector was kindly provided by F. Benzanilla from the University of Chicago. *Escherichia coli* strains M15 and SG1300 and plasmid vectors pQE32 and pQE70 were purchased from Qiagen (Valencia, CA). Penta-His and RGS-His antibodies were purchased from Qiagen. The GST antibody was purchased from GE Healthcare. IPTG and the detergents were obtained from Anatrace (Maumee, OH). Talon cobalt resin was purchased from Clontech (Mountain View, CA). The reducing agent TCEP was purchased from Pierce (Rockford, IL). The reducing reagent TCYP, along with the fluorophores fluorescein 5-maleimide and tetramethylrhodamine 5-maleimide, were purchased from Molecular Probes (Carlsbad, CA). The spin-label (1-oxyl-2,2,5,5-tetramethylpyrrolidin-3-yl) methyl methanethiosulfonate was purchased from Toronto Research Chemicals (North York, ON). The lipids POPC, POPE, and POPG, *E. coli* polar lipid extract, chicken egg extract, and soy bean extract asolectin were purchased from Avanti Polar Lipids (Alabaster, AL). All other reagents were purchased from Sigma or Fisher.

Molecular Biology and Expression Test. The DNA fragment containing the first 260 amino acids of the voltage-sensing domain of Ci-VSP [Ci-VSD-1−260 (Figure 1A)] was amplified by polymerase chain reaction and cloned into pET28b, pQE32, pQE70, and pGEX-6p-1 vectors. The pET28b vector was premodified into two individual vectors that contain one His tag at either the N- or C-terminus. The Ci-VSD-containing plasmids were transformed into fresh *E. coli* competent cells and grown overnight at 37 °C for 12−16 h. The saturated overnight cultures were diluted at a 1:100 ratio into LB medium with 1% glycerol and grown at 37 °C for 2−4 h, and expression was induced at an OD_{600} of ∼1 with 1 mM IPTG for 3 h at 37 °C. Cell samples (1 mL) were collected before induction and at the end of the expression run. Cells were spun down and the pellets resuspended in SDS loading dye. Viscous samples were broken down by shear force with a

dx.doi.org/10.1021/bi300980q | *Biochemistry* 2012, 51, 8132−8142

syringe fitted with a 30 gauge needle. SDS-dissolved cell samples were loaded for sodium dodecyl sulfate−polyacrylamide gel electrophoresis (SDS−PAGE) and developed for Western blotting. The penta-His antibody was used as primary antibody for pET28b and pQE32, the RGS-His antibody for pQE70, and a GST antibody for pGEX-6P-1. In all cases, the secondary antibody was anti-mouse Alexa fluor 647, followed by detection on a ChemiDoc (Bio-Rad). Expression levels were compared roughly by intensity from Western blots. Initial expression conditions were further optimized for *E. coli* strain, temperature, IPTG amount, and expression time, following the procedures described above.

The only native cysteine residue at position 159 was mutated to a serine by site-directed mutagenesis methods following standard procedures to give a cysteine-less Ci-VSD, which was used as a template to generate a single-cysteine mutant for probing methods with fluorescence or EPR spectroscopy. A total of 44 plasmids, each with a single cysteine residue scanning positions 110−142 and 214, were prepared on the optimized expression construct as described below.

Expression and Purification of Ci-VSD. Fresh XL10-Gold competent cells were transformed with Ci-VSD-1−260 in pQE32. The transformation mixture was grown overnight in the presence of 100 mg/L ampicillin. Overnight cultures were diluted 1:100 in regular LB medium in the presence of 0.2% glucose. Cells were grown at 37 °C for 3−4 h to an OD_{600} of 0.5−0.7, and protein expression was induced with 0.65 mM IPTG for 3 h at 30 °C. The cells were harvested by centrifugation, and the pellet was resuspended in Tris buffer [20 mM Tris (pH 8.0) and 150 mM NaCl] in the presence of 1 mM phenylmethanesulfonyl fluoride (PMSF), 0.1 mg/mL DNase, 5 mM $MgCl_2$, 0.1 μg/mL pepstatin, 1 μg/mL aprotinin, and 1 μg/mL leupeptin. The mixture was homogenized and spun down at 100000*g* for 35 min, and the membrane fraction was resuspended in Tris buffer and solubilized with 10 mM Anzergent 3-14 in the presence of 1 mM PMSF, 5 mM imidazole, and 1 mM β-mercaptoethanol at room temperature for 1 h. The homogenate was then spun down at 100000*g* for 35 min, and the supernatant was loaded onto a cobalt metal-affinity resin (2 mL of resin/L of cell culture). The resin was washed with 20 resin volumes of Tris buffer in the presence of 1 mM Anzergent 3-14 and 5 mM imidazole. Ci-VSD was eluted with 300 mM imidazole in the presence of 1 mM Anzergent 3-14 and Tris buffer (pH 8.0). For the purification of single-cysteine mutants, all washing buffers contained additional 0.5 mM tris(2-carboxyethyl)phosphine hydrochloride and 0.5 mM tris(2-cyanoethyl)phosphine. The eluate from the cobalt column was further purified by size exclusion chromatography (SEC) using a Superdex 200 HR 10/30 column (GE Healthcare) in an AKTA FPLC system from the same company.

Detergent Screen. All detergents were from Anatrace and of the highest purity. Following the methods described above, the *E. coli* pellet containing the membrane fraction, from a large-scale Ci-VSD expression, was resuspended in Tris buffer as crude membranes. Fourteen detergents were individually added to the membrane suspension at 10 times their critical micelle concentration. After a 3 h solubilization at room temperature, the mixture was centrifuged at 100000*g* for 1 h. The pellet was completely dissolved in SDS loading dye to the same initial volume, and both the supernatant and the dissolved pellet were subjected to SDS−PAGE and detected by Western blotting. The efficiency of extraction of Ci-VSD from the membrane was estimated by the relative amount of protein in the supernatant fraction over the pellet fraction.

After Ci-VSD had been extracted from *E. coli* membranes, the solubilization detergent was exchanged with 18 detergents to evaluate Ci-VSD's homogeneity. The Superdex 200 HR 10/30 column was individually pre-equilibrated with various detergents, and ∼0.2 mg of Ci-VSD from the cobalt column eluate was loaded for SEC. Peak homogeneity was calculated with the UV elution profile by the ratio of the weighted 1 mL main peak to the weighted entire protein elution region using the following equation:

$$\text{probability of homogeneity} = \frac{(\int_{Vp-0.5}^{Vp+0.5} A\ dV)/(\int_{Vp-0.5}^{Vp+0.5} dV)}{(\int_{Vv}^{Ve} A\ dV)/(\int_{Vv}^{Ve} dV)}$$

where A is the UV absorbance at 280 nm, Vp is the elution volume of the main peak that is between 13.5 and 14.2 mL for all tested detergents, Vv is the void volume of the column (7 mL), and Ve is the end volume (17 mL) for the protein-related absorbance in the elution profile. Peak homogeneity from Vp − 0.5 mL to Vp + 0.5 mL was calculated for each elution profile for 18 detergents. Detergents with top homogeneity probabilities were selected to test for stability at high concentrations.

For stability determination, Ci-VSD was purified with the chosen detergents and concentrated to 20 mg/mL (∼600 μM). Protein samples were kept at room temperature (∼22 °C) for a week and their concentrations monitored by UV−visible spectroscopy (Nanodrop, Thermo Scientific) using 32430 M^{-1} cm^{-1} as the extinction coefficient, following sample filtering through a centrifuge filter with a pore size of 0.22 μm, to remove potential aggregates. After a week, the remaining protein samples were loaded back onto the SEC system to check their homogeneity. Detergents that kept Ci-VSD homogeneous at 20 mg/mL for a week were considered compatible with subsequent high-resolution structural studies.

Protein Characterization. The purity of Ci-VSD was established by SDS−PAGE, while its secondary structure in detergent was determined by circular dichroism (CD) spectroscopy. The protein concentration was adjusted to ∼10 μM, and the spectra were measured on a model 202 AVIV circular dichroism spectrophotometer (AVIV Instrument Inc.) between 190 and 260 nm in 1 nm intervals in a 1 mm path length strain-free cylindrical cuvette (Hellma, Jamica, NY). The differential absorbance was converted into molar ellipticity [θ]. The percent helicity of Ci-VSD was calculated from θ_{222} following standard methods.[22]

The molecular mass and homogeneity of Ci-VSD−detergent complexes were determined by multiple-angle light scattering (MALS) methods. An AKTA FPLC system equipped with a Superdex 200 HR 10/30 size exclusion column was coupled to a MALS system with a flow cell. Light scattering was detected with a HELEOS system (Wyatt Technology Corp.) equipped with a 60 mW GaAs laser at 658 nm and 18 detectors at angles from 22.5° to 147.0°. The refractive index was determined from an Opilab rEX unit (Wyatt Technology Corp.). The refractive index increment (dn/dc) of Anzergent 3-14 was determined by a linear fit of its refractive indexes at incremental concentrations to be 0.1534 mL/g. The UV absorbance was measured at 280 nm by the detector from the AKTA system (GE Healthcare) and converted to analog between 0 and 1 V into the HELEOS system. Data were acquired and analyzed using the ASTRA

Table 1. *E. coli* Strains and Constructs for the Initial Expression Test[a]

sequence	affinity tag	vector	promoter	*E. coli* strain	expression level
Ci-VSD-1−260	N-terminal His tag	pET28b	T7	BL21 DE3	+
				BL21 DE3 pLysS	[++]
	C-terminal His tag	pET28b	T7	BL21 DE3	−
				BL21 DE3 pLysS	−
	C-terminal His tag	pQE70	T5	XL1-Blue	−
				XL10-Gold	−
	N-terminal His tag	pQE32	T5	XL1-Blue	++
				XL10-Gold	[+++]
	N-terminal GST tag	pGEX-6P-1	LAC	BL21 DE3	+
				XL1-Blue	−

[a]Positive (+) and negative (−) signs indicate the relative expression level from Western blot: −, no visible band of expression; +, visible band. Multiple signs indicate relatively higher expression levels. The two conditions from the initial test shown in brackets were chosen for further optimization for expression.

software package (Wyatt Technology Corp.). Even though self-correlation between the intensity of light scattering at discrete angles is sufficient to determine the molecular mass without a standard, a BSA sample was used to ensure correct settings and data analysis. Both the molecular mass of the protein−detergent complex and the protein content of the complex were analyzed for the peak of interest by the system template Protein Conjugate of ASTRA.

Reconstitution and Fluorescence Spectroscopy. Ci-VSD was reconstituted into liposomes with five different compositions: asolectin, *E. coli* extract, chicken egg extract, 3:1 POPE/POPG liposomes, and 3:1 POPC/POPG liposomes. The degree of aggregation of Ci-VSD in liposomes was determined by an established fluorescence energy transfer method.[23−25] Liposomes were prepared from stock lipids in chloroform following standard protocols[26] in 10 mg/mL stock solutions. Concentrated Ci-VSD (∼5 mg/mL) samples were incubated with stock liposomes for 30 min. The mixture was diluted 20 times, and detergents were removed using biobeads (Bio-Rad) overnight at room temperature.

Ci-VSD G214C was purified and individually labeled with either fluorescein 5-maleimide (excitation_{max} = 494 nm; emission_{max} = 518 nm) or tetramethylrhodamine 5-maleimide (excitation_{max} = 544 nm; emission_{max} = 572 nm) fluorescence dye. The individually labeled Ci-VSD G214C was mixed at a 1:1 donor:acceptor ratio and reconstituted into liposomes. The fluorescence emission was recorded from 500 to 650 nm while excited at 494 nm in a PTI fluorimeter (PTI Technology). The relative FRET intensity in the 570−580 nm range was used as an indicator of the closeness between the donor and acceptor and, thus, the relative aggregation level of Ci-VSD. Lipid compositions, protein:lipid ratios and the stability versus time were tested and optimized for minimal FRET values.

EPR Spectroscopy. Ci-VSD single-cysteine mutants were purified and spin-labeled using a 1:20 molar excess of spin-label at room temperature for 20 min. Excess spin-label was removed with a PD10 column (GE Healthcare). After liposome reconstitution, continuous-wave (CW) EPR measurements were taken following the standard protocol.[23,25,27] The mobility (ΔH_o^{-1}), Ni-EDDA accessibility (ΠNi), and oxygen accessibility (ΠO_2) were obtained to deduce the dynamic and structural information about Ci-VSD inside the liposome. Periodic analysis was done following standard methods.[27] Briefly, the oscillation of ΠO_2 along the residue number was Fourier transformed into an angular power spectrum $P(\phi)$ in the range of 1−180°. The ideal α-helix (3.6 residues per turn) is expected to have a maximal peak around 360°/3.6 = 100° with a weighted probability αPI of >2.

To determine the directionality of Ci-VSD reconstitution in liposomes, we followed the percentage of quenching on the spin-label signals at two positions, 110 and 141, on the opposite sides of the membrane. Ci-VSD 110C and 141C were labeled with spin-label and reconstituted into multiple-layer liposomes, which was the standard procedure for EPR. Reconstituted unilamellar proteoliposomes were generated by extrusion (30 times) through a 100 nm polycarbonate double membrane (Avanti Polar Lipids). Samples (20 μL) were loaded onto sealed glass capillaries, and CW-EPR spectra were measured with a high-Q cavity (Bruker Biospin). The impermeable spin-label quencher potassium tris(oxalato)chromate(III) (CrOx) was used to evaluate VSD orientation. Because of its high charge (+3), chromium(III) essentially cannot permeate the lipid bilayer. The percent reduction of the peak amplitude of Ci-VSD in the presence and absence of 30 mM CrOx directly indicates the amount of spin-label on the outside surface of the liposome. For the method to be internally consistent, two opposite sides on each Ci-VSD surface should have complementary quenching percentages.

RESULTS

Protein Expression. During initial expression tests, five of seven Ci-VSD-1−260 constructs were successfully expressed in *E. coli* strains (Table 1). The two best expressors (highlighted in Table 1) were further optimized by exploring *E. coli* strains, temperature, IPTG concentration, and expression time. Expression conditions were tested for the N-His-Ci-VSD-260 in pET28b construct in four different BL21 DE3 strains: BL21 DE3, BL21 Gold DE3, BL21 codon + RPIL, and BL21 DE3 pLysS; construct Ci-VSD-1−260-C-His in pQE32 was tested in five different *E. coli* strains: XL10-Gold, XL1-Blue, DH5a, M15, and SG1300. The two best conditions were used for preparative scale expression and optimized with regard to purity and yield. The two best outcomes from expression tests occurred for N-His-Ci-VSD-1−260 in pET28b in BL21 Gold, induced by 1 mM IPTG for 6 h at 37 °C, and Ci-VSD-1−260-C-His in pQE32 in XL10-Gold, induced with 0.65 mM IPTG for 3 h at 30 °C.

Protein Purification. Preparative expression (1 L culture) of Ci-VSD was conducted with the two established constructs and conditions described above. The cells were harvested and homogenized, and the supernatant was discarded after centrifugation at 100000*g* for 35 min. The pellet was

dx.doi.org/10.1021/bi300980q | *Biochemistry* 2012, 51, 8132−8142

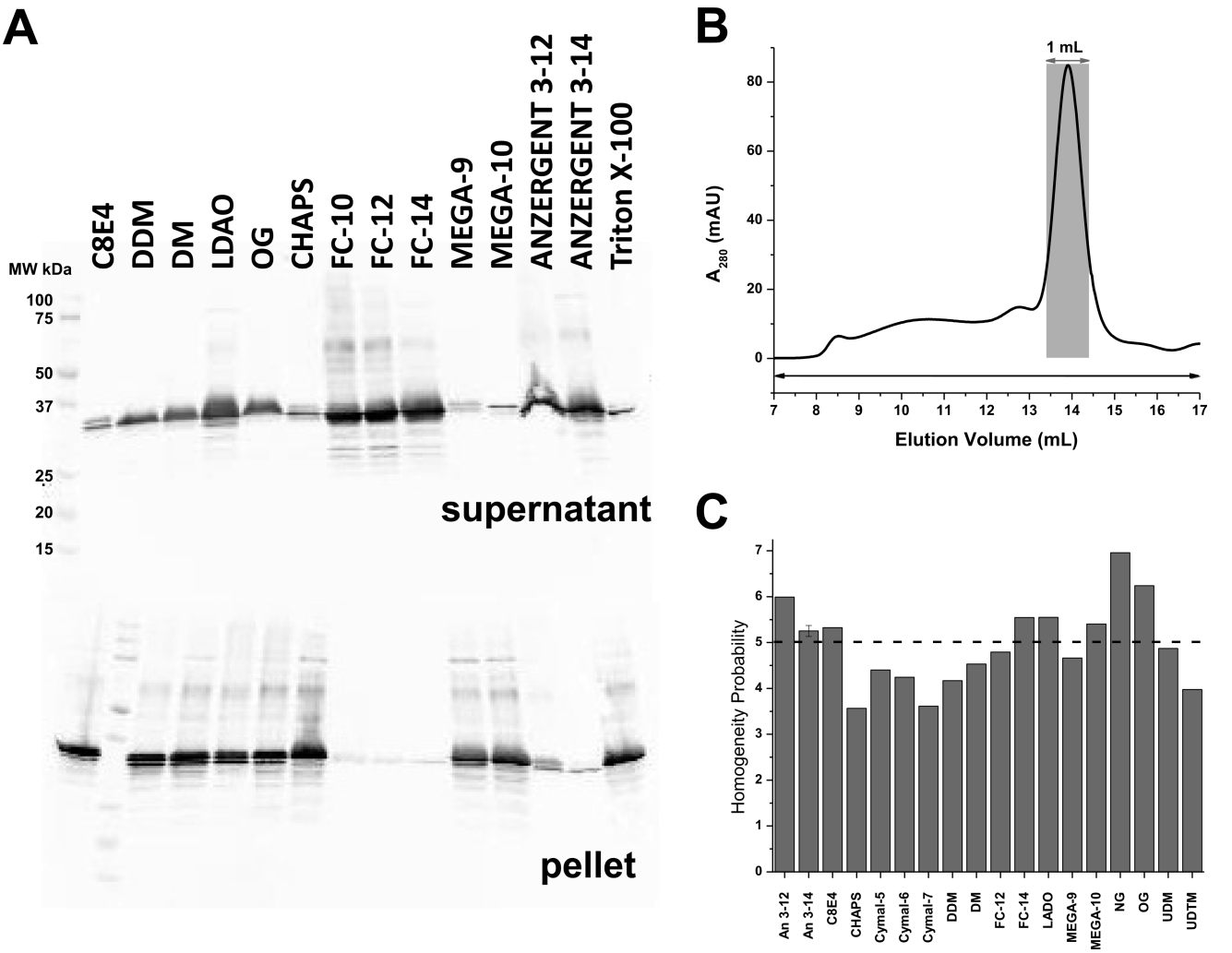

Figure 2. Detergent screen. (A) Western blot of solubilization test: (top) supernatant fractions extracted by different detergents after ultracentrifugation and (bottom) pellet fraction dissolved in SDS. FC-10, FC-12, FC-14, Anzergent 3-12, and Anzergent 3-14 were able to extract Ci-VSD efficiently out of crude cell membranes. FC-12 and Anzergent 3-14 were chosen for the subsequent purification test. (B) Representative elution profile of the crude eluate from cobalt affinity chromatography via SEC with Anzergent 3-14. Its elution volume is 13.7 mL on the Superdex 200 HR 10/30 column. The homogeneity of the main peak was calculated from the ratio of the weighted main peak (gray area) to the weighted whole region (black double-headed arrow at the bottom). (C) Homogeneity probability of Ci-VSD eluted in 18 detergents. Eight detergents (Anzergent 3-12, Anzergent 3-14, C_8E_4, FC-14, LDAO, Mega-10, NG, and OG), whose homogeneity probability is higher than the reference line (---), were chosen for the additional stability test.

resuspended in Tris buffer as crude membranes. Solubilization with 5 of 14 screened detergents (FC-10, FC-12, FC-14, Anzergent 3-12, and Anzergent 3-14) allowed extraction of >90% of the Ci-VSD into the supernatant fraction from the crude membrane (Figure 2A, top). No obvious protein degradation was observed during the solubilization stage judged by Western blots. FC-12 and Anzergent 3-14 were chosen for the solubilization of larger-scale expression and further optimization test of the protein's purity, homogeneity, and stability. After the cobalt affinity column and SEC purification, SDS–PAGE was used to determine purity. N-His-Ci-VSD-1–260 in pET28b expressed in BL21 Gold shows significant amounts of impurities seen as multiple bands via SDS–PAGE after purification (data not shown). On the other hand, Ci-VSD-1–260-C-His in pQE32 expressed in XL10 Gold gives a suitable purity under the same conditions. Figure 3A shows an overloaded SDS–PAGE gel of Ci-VSD-1–260-C-His in the pQE32 construct that amplifies the impurities and demonstrates the purity resulting from the optimized procedures.

Protein Characterization. On the basis of SDS–PAGE (Figure 3A), the molecular mass of the Ci-VSD-1–260-C-His construct was 28 kDa determined by the R_f value in reference to a marker (analysis not shown). This is slightly lower than its predicted molecular mass of 31.0 kDa and probably indicates that Ci-VSD retains at least partial secondary structure in SDS. This observation is not uncommon among membrane proteins.[28]

Ci-VSD's homogeneity and stability were screened by SEC by loading the protein samples into columns pre-equilibrated with Tris buffer and 18 individual detergents (Figure 2C). We report an elution volume of 13.7 mL in Anzergent 3-14 using a Superdex 200 HR 10/30 column (Figure 2B). The elution profiles for Ci-VSD in other detergents all contained predominant peaks around 13.4–14.2 mL but displayed different amounts of high-molecular mass components at 7–12 mL (void volume of ~8.5 mL). Ranked by the homogeneity probabilities, the eluted proteins were collected from the top eight detergents (above the dotted line in Figure 2C) and

dx.doi.org/10.1021/bi300980q | *Biochemistry* 2012, 51, 8132–8142

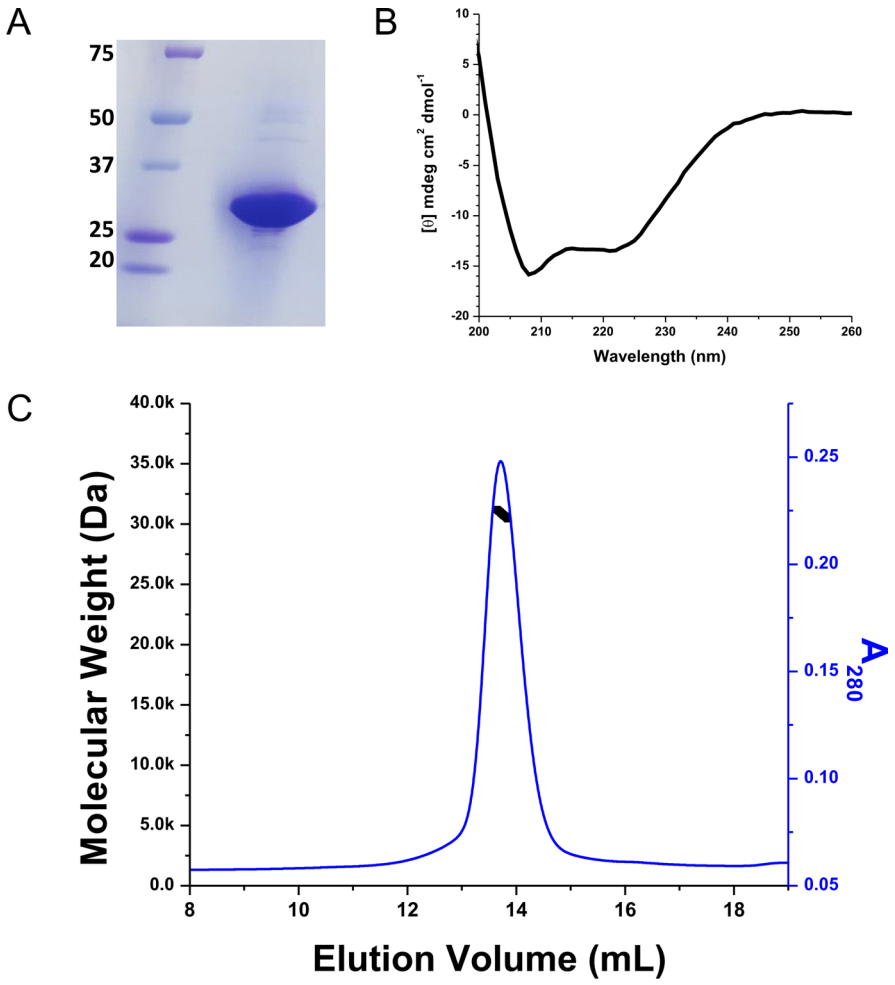

Figure 3. Ci-VSD characterization. (A) SDS–PAGE gel of Ci-VSD-1–260. The sample was overloaded to amplify the impurities. (B) Circular dichroism spectra in molar ellipticity of Ci-VSD in Anzergent 3-14. The calculated helicity is 52%, which is consistent with high helical contents for the expected four transmembrane helices. It suggests that Ci-VSD maintained its secondary structure in the tested detergent and the N-terminal region of residues 1–100 is most likely unstructured. (C) Ci-VSD's molecular mass determined by multiple-angle light scattering methods in Anzergent 3-14. The molecular mass (black line) is evenly distributed throughout the peak region (blue line), indicating a homogeneous protein–detergent complex.

concentrated to ~20 mg/mL. The protein concentration was monitored after removal of potential aggregation with a 0.22 μm filter. Ci-VSD continually precipitated in MEGA-10, NG, and OG at high concentrations but became stable at concentrations of <1 mg/mL. The rest of the five concentrated samples were reloaded onto the SEC instrument after a week, with the aggregation portion increasing slightly and the predominant peak representing >90% of the homogeneous protein. Criteria on homogeneity and stability determined a list of five detergents (Anzergent 3-12, Anzergent 3-14, C_8E_4, FC-14, and LDAO) that are compatible with Ci-VSD at a high concentration (20 mg/mL). Anzergent 3-14 was chosen for all subsequent sample preparations.

The homogeneity of the molecular mass was further evaluated by multiple-angle light scattering after SEC separation of the main peak region. The determined molecular mass of the Ci-VSD–Anzergent 3-14 complex is 77.8 kDa; 39% of that corresponds to the protein fraction. The molecular mass of Ci-VSD was determined to be 30.3 kDa evenly distributed throughout the main peak (Figure 3C). This indicates that Ci-VSD is a stable monomer in complex with approximately 130 Anzergent 3-14 molecules at the analyzed concentration of ~0.5 mg/mL. The molecular mass and homogeneity of Ci-VSD analyzed with three other detergents (OG, LDAO, and DM) were also similar to those with Anzergent 3-14.

We then evaluated the secondary structure of Ci-VSD in Anzergent 3-14 by CD spectra. The spectra show the typical features of the α-helical conformation (Figure 3B) with ellipticity minima near 208 and 222 nm. On the basis of standard basis set spectra, the calculated helical content of Ci-VSD is 52%. As expected, this points to a predominately helical conformation for Ci-VSD in detergent and is consistent with the four transmembrane helices within residues 100–239 predicted by sequence alignment. The N-terminal region of the first 100 residues seems to be unstructured under these conditions. These results suggest that the transmembrane region of Ci-VSD folds well in detergent, appears to be stable, and displays the characteristic secondary structure profile of all reported VSDs.

Reconstitution, Stability, and Orientation. Membrane proteins have a tendency to form small aggregates under nonphysiological conditions. This crowding effect is usually more dramatic when the proteins are reconstituted into bilayers and limited in two-dimensional space or as a consequence of

dx.doi.org/10.1021/bi300980q | *Biochemistry* 2012, 51, 8132–8142

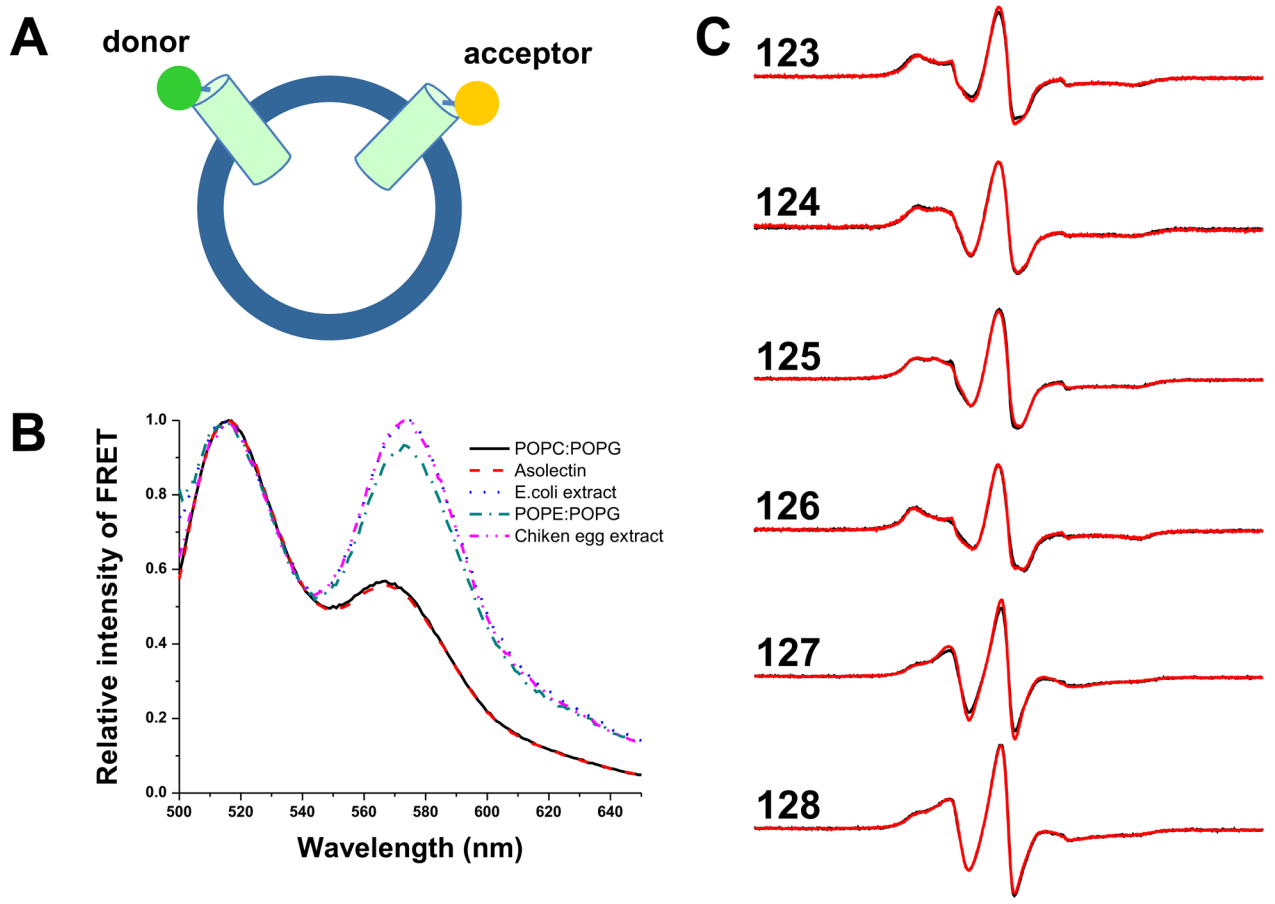

Figure 4. Ci-VSD reconstitution. (A) Cartoon representation of the FRET assay for evaluating the aggregation behavior. Ci-VSD was individually labeled with the fluorescence donor and acceptor, mixed at a 1:1 molar ratio, and reconstituted into liposomes. The FRET signal in the range of 560−580 nm indicates of closeness of fluorophores in liposomes and, thus, the degree of Ci-VSD aggregation. (B) FRET signal of Ci-VSD in five different liposomes at a 1:2000 protein:lipid ratio 24 h after reconstitution. The magnitudes of the signals from 3:1 POPC/POPG liposomes and asolectin were significantly lower than those for the other three compositions. (C) CW-EPR spectra of Ci-VSD in POPC/POPG liposomes (red) and asolectin (black) at six residues (123−128) in the first transmembrane segment (S1). Spectral features are distinctly different among residues, but essentially the same in both liposomes.

hydrophobic mismatch.[29] Most local dynamics and solvent accessibility measurements rely on the protein being monodisperse on the plane of the lipid bilayer. In addition, the voltage-dependent response of VSDs is known to be sensitive to lipid composition.[30−32]

On the basis of single-molecule fluorescence approaches, Ci-VSP has been shown to be monodisperse in its functional state after heterologous expression in *Xenopus* oocytes.[33] We conducted a systematic search for reconstitution conditions that afforded Ci-VSD monodispersity in liposomes. To that end, Ci-VSD was reconstituted into premade liposomes of five different compositions: asolectin, *E. coli* extract, chicken egg extract, 3:1 POPE/POPG liposomes, and 3:1 POPC/POPG liposomes. The extent of two-dimensional aggregation was estimated by a simple FRET-based assay (Figure 4A) in which a single-cysteine mutant of the test protein was alternatively labeled with donor or acceptor fluorophores.[23−25] Ci-VSD mutated at position 214 (G214C) was expressed and individually labeled with a fluorescence donor and an acceptor (fluorescein/tetramethylrhodamine pair), mixed at a 1:1 ratio, and reconstituted into different liposomes with a 1:2000 protein:lipid molar ratio. The FRET signal was monitored after reconstitution for 24 h. Magnitudes of FRET signals in the range of 570−580 nm were significantly lower in POPC/POPG liposomes and asolectin (Figure 4B), which indicates that Ci-VSD is monodisperse under those conditions. The protein:lipid ratio and Ci-VSD's stability over time were also tested (data not shown). Ci-VSD did not show a significant increase in the magnitude of the FRET signal in either POPC/POPG liposomes or asolectin at a protein:lipid molar ratio of ≤1:250 within 48 h at room temperature.

To compare the effect of lipid composition on Ci-VSD conformation in lipids, we conducted limited site-directed spin labeling on six residues (123−128) in the first transmembrane segment (S1) of Ci-VSD under two different conditions: POPC/POPG liposomes and asolectin. The spin-labeled cysteine mutants were subjected to CW-EPR spectroscopic measurements on liposomes in the absence of a nominal transmembrane voltage. These conditions stabilize Ci-VSD in its resting conformation. In Figure 4C, the EPR spectra show the expected difference among residues scanned along a single helix of the four-helix bundle. However, this sequential pattern is independent of whether the measurement is taken in asolectin or POPC/POPG liposomes (Figure 4C), as expected from a well-behaved nonaggregated reconstituted sample. Given that earlier EPR studies from this laboratory have been conducted using POPC/POPG mixtures for KvAP[23,25] and

dx.doi.org/10.1021/bi300980q | *Biochemistry* 2012, 51, 8132−8142

NaChBac[34] voltage sensors, all subsequent spectroscopic studies were also conducted in this lipid mixture.

Transduction of the electric field energy by VSDs is, by necessity, vectorial in nature. Therefore, in planning and interpreting spectroscopic data from reconstituted protein, we found it is of paramount importance to determine whether an external electric field is applied to a molecule population that has been vectorially reconstituted or one that displays a random orientation. In the first case, the ensemble will respond synchronously, and any resulting signal corresponds to one (or very few) conformational state. The second case generates a mixed and complicated signal mix composed of at least a fraction of the population that responds to the external electric field and a presumably unresponsive fraction. The Ci-VSD reconstitution orientation was determined using the ability of certain paramagnetic metals to quench (broaden) nitroxide signals in a collision-dependent way. Chromium(III) oxalate (CrOx) is one of the most effective paramagnetic relaxing reagents and, because of its net charge (+3), essentially cannot permeate a lipid bilayer.[35] We determined the fractional quenching by the amplitude reduction of CW-EPR signals in Ci-VSD spin-labeled at two positions, 110 and 141, on the opposite sides of the membrane. Spin-labeled sensors were individually reconstituted into POPC/POPG liposomes and quenched with 30 mM CrOx. We find that the reduction of the peak amplitude was, on average, 36% for position C110 and 44% for position C141 (Figure 5B). Because C110 and C141

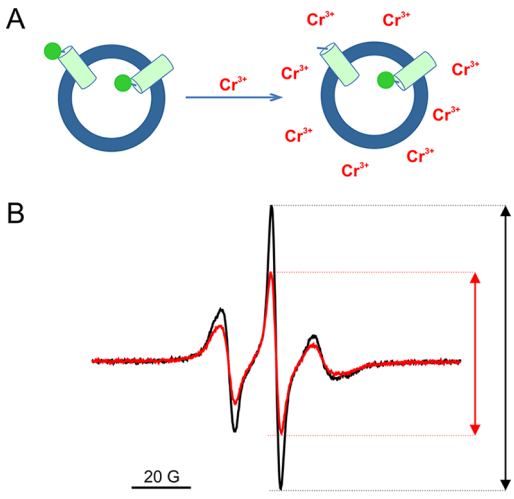

Figure 5. Direction of Ci-VSD in liposomes. (A) Cartoon representation of chromium(III) quenching methods for accessing the direction of Ci-VSD in liposomes. Addition of 30 mM CrOx to the exterior solution will quench the spin-label signal at the outside surface of the liposome. The percent of quenching illustrates the direction of the labeled position in reference to the liposome: inside, outside, or randomly distributed. (B) Spectra of spin-labeled Ci-VSD C141 in POPC/POPG liposomes (black) and in the presence of 30 mM CrOx (red). The percent of amplitude reduction is 44%.

are on the opposite sides of the bilayer (Figure 6A, top), the percent of quenching should be complementary. Under these conditions, if sensors are randomly reconstituted, the theoretical values for quenching would be close to 50%, but close to either 0 or 100% for a fully vectorial reconstitution. The values for C110 and C141 were clearly closer to 50% in both our samples, unambiguously suggesting that Ci-VSD reconstitution shows little vectoriality. The ~10% discrepancy was likely from the imperfect sample preparation and partial shielding effect from the liposome, which could somewhat reduce the efficiency of collision between the spin-label and CrOx.

Local Structure and Dynamics. Once conditions were established to reliably generate a stable, well-behaved, reconstituted Ci-VSD preparation, we initiated an exploration of the overall structure and dynamics of the sensor in liposomes. As an initial approximation, we conducted a series of sequential cysteine mutations in the first transmembrane segment, S1, and the adjacent extracellular loop [residues 110–142 (Figure 6A)]. Each of these cysteines was subsequently spin-labeled, and their CW-EPR spectra were measured to characterize their local environmental properties: local dynamics from mobility measurements (ΔH_o^{-1}) and accessibility to contrast agents Ni-EDDA (ΠNi) and oxygen (ΠO_2). ΔH_o^{-1} is an empirical measure of the local dynamics of the labeled site, by the spectral anisotropy affected through tertiary contacts. ΔH_o^{-1} is expected to be higher at loop regions and oscillate in transmembrane regions involved in periodic tertiary interactions between lipids and other parts of the protein. Ni-EDDA is a water-soluble chelated paramagnetic ion and reflects accessibility to extramembrane aqueous environments. ΠNi is expected to be high for exposed loop regions but extremely low or absent for transmembrane regions. In contrast, O_2 shows higher solubility in lipids, so that high ΠO_2 reflects lipid-exposed regions.

Residues 110, 111, 140, and 141 clearly displayed high Ni-EDDA accessibilities as is characteristic of water-exposed regions, while positions 113–139 show very limited water accessibility (Figure 6B, top, gray region). These data unambiguously define the boundary of the membrane-embedded boundaries of the first transmembrane region, fully consistent with the expected range for the S1 segment from sequence alignments. The ΠO_2 and ΔH_o^{-1} values, on the other hand, show clearly periodic behavior with maximal values every three or four residues, confirming its α-helical secondary structure. As a comparison, the previously determined ΠO_2 of the KvAP S1 segment was plotted and aligned with our Ci-VSD data. The values of ΠO_2 show general agreement with regard to range and oscillation pattern. The periodicity of the ΠO_2 oscillation within residues 113–138 can be quantitatively analyzed by evaluating its angular power spectrum after a Fourier transform.[27] Figure 6C shows the power spectrum from the ΠO_2 oscillation data in Figure 6B. The angular periodicity probability is characterized by a single dominating peak around 105°, close to the ideal α-helix value of 100°. The α-helical probability (αPI = 3.5 > 2) also points to the strong helicity of the S1 segment. Overall, this data set strongly supports the idea that the S1 region of Ci-VSD folds in the same way and in a similar conformation as that of the structurally characterized KvAP sensor.

DISCUSSION

The mechanism of voltage sensing remains one of the most challenging subjects in modern biophysics. Several models have been proposed to explain the mechanism of voltage sensing.[36,37] With recent advances in membrane protein crystallography, structures of voltage-gated ion channels are being determined at an unprecedented rate,[14,16−18] yet because these are biochemically processed membrane protein samples, all available structures have been determined in the absence of a nominal transmembrane electric field. Perhaps, not surprisingly,

dx.doi.org/10.1021/bi300980q | Biochemistry 2012, 51, 8132−8142

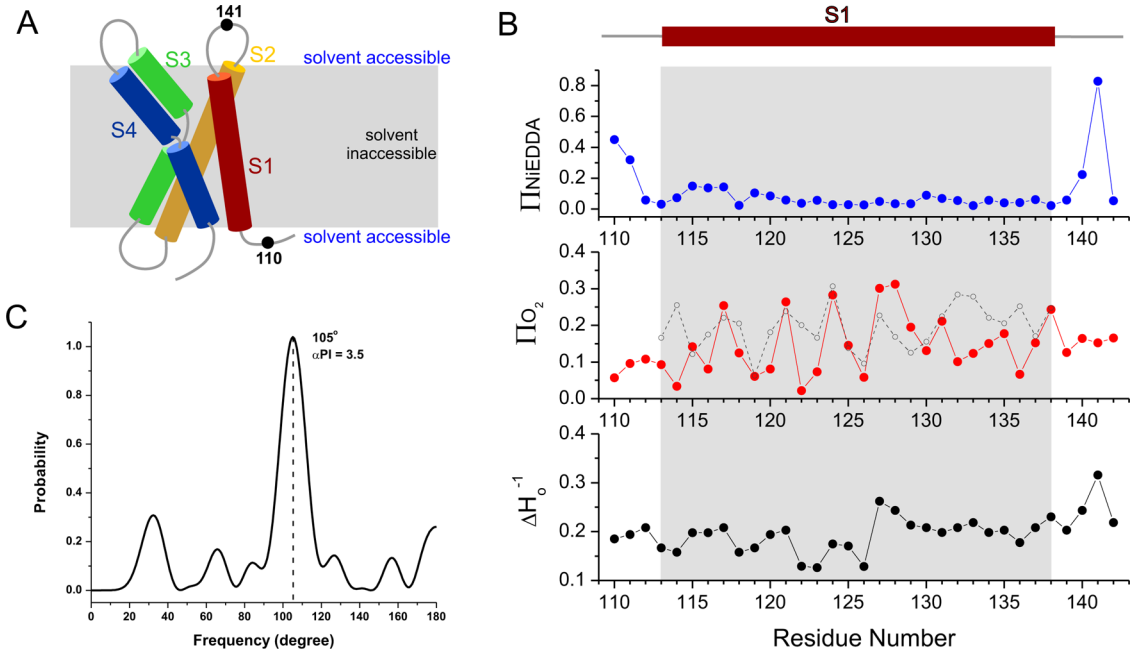

Figure 6. Structure of S1 of Ci-VSD in liposomes studied by EPR spectroscopy. (A) Cartoon representation of VSD's scaffold of four helices. The relative position of the membrane is shown in gray, where it is solvent inaccessible. Positions 110 and 141 are outside of the lipid bilayer and on the opposite sides. (B) Ni-EDDA accessibility (ΠNi, blue), oxygen accessibility (ΠO_2, red), and mobility (ΔH_o^{-1}, black) for S1 of Ci-VSD. The gray region represents the transmembrane region identified by ΠNi. The ΠO_2 values of KvAP in the homologous region are plotted in gray as a reference. Two sets of ΠO_2 values oscillate in the same range with almost the same pattern, with maximal values every three or four residues. They indicate that S1 of Ci-VSD folds into an α-helix in liposomes in the same way as KvAP. Clearly, Ci-VSD folds into the same scaffold as existing VSDs. (C) Periodic probability analysis of ΠO_2 of the transmembrane region of residues 113−138 shows a P_{max} of 105° and an αPI of 3.5. It suggests the α-helical conformation has 3.4 residues per turn (360°/105°) with high probability (αPI > 2).

all of the available VSD structures appear to converge on one stable conformation, that of the activated or Up state. The discovery of VSD-linked phosphatases like Ci-VSP[3] has not only demonstrated the universality of the VSD scaffold as a means of electromechanical coupling but also might offer an alternative for pursuing multiple VSD conformations using structural approaches.

In reference to VSDs from canonical voltage-gated ion channels, the voltage-dependent behavior of Ci-VSP is unique in two clear ways. First, its voltage dependence is significantly right shifted. Second, it shows a much shallower activation slope (z = 1−2), suggesting that less charge might be transferred during the gating process. These properties indicate that under biochemical conditions (close to 0 mV) most of the Ci-VSD molecules would populate the resting or Down state. Consequently, a viable Ci-VSP biochemical preparation would provide access to alternative VSD conformations using high-resolution structural approaches.

As an initial approximation, we have focused efforts on developing a bacterial expression system for the eukaryotic Ci-VSD. Expression tests included constructs containing a combination of bacterial promoters (T7, T5, and LAC) and affinity tags (N-terminal His tag, C-terminal His tag, and GST tag) in various *E. coli* strains (BL21 DE3, BL21 pLysS, XL-Blue, and XL-Gold). Early tests successfully showed that Ci-VSD could be overexpressed in *E. coli*. Fourteen detergents were screened by their ability to extract the most protein from the crude membrane, while 18 detergents were screened for Ci-VSD's homogeneity and stability. Here, we show that Ci-VSD can be purified to homogeneity after a simple two-step purification through cobalt affinity chromatography and size exclusion chromatography. The yield of our final optimized protocol is ∼0.5 mg/L of culture with the detergent Anzergent 3-14.

The native environment for membrane proteins is defined by a complex interplay between lipid composition and the local physical properties of the membrane. The topology and three-dimensional architecture determinations of membrane proteins by spectroscopic approaches rely on the fact that proteins have to be monodisperse on the plane of the bilayer; otherwise, the acquired information will be blended by the effect of nonspecific protein−protein contacts. Using a simple FRET assay, we showed Ci-VSD can be reconstituted as a monomer using various phospholipid compositions and following standard procedures. However, the relative FRET signals were shown to be quite different for different tested liposomes, suggesting that the aggregation behavior of Ci-VSD is very sensitive to lipid composition. Ci-VSD is remarkably stable in POPC/POPG and asolectin liposomes. Puzzlingly, while Ci-VSD can be overexpressed in *E. coli*, it severely aggregates in *E. coli* lipid extract. It should be noted that membrane protein handling might not be well-defined under overexpression conditions, thus emphasizing the necessity for lipid composition screens as a prerequisite to structural or functional assays.

Under physiological conditions, membrane proteins are anchored to lipid bilayers in a preferred direction and respond to specific stimuli from both sides of the membrane. This is particularly relevant when the external stimulus is vectorial in nature, as is the case for the transmembrane electric fields. Establishing the overall orientation of Ci-VSD after reconstitution is of utmost importance, for it defines the types of experimental approaches that can be pursued to determine voltage-driven conformational changes. Our current results from ΠNi determinations and enhanced paramagnetic

dx.doi.org/10.1021/bi300980q | *Biochemistry* 2012, 51, 8132−8142

relaxation methods indicated that, as is the case for many voltage-gated channels or isolated VSDs, Ci-VSD reconstitutes essentially in a random orientation. For spectroscopy-based approaches, this result limits experiments to measurements in the absence of an external transmembrane voltage. However, other liposome preparation and reconstitution protocols will need to be further developed and optimized if external transmembrane voltages are to be applied on the proteoliposome population.

The fact that the purified and reconstituted Ci-VSD preparation represents a properly folded and structurally stable system was demonstrated by limited site-directed spin labeling analysis of the first transmembrane segment (S1). We focused on this region, as it tends to be structurally conserved among all available VSD structures. Local environmental parameters reflecting overall dynamics (ΔH_o^{-1}), accessibility to the lipid environment (ΠO_2), or accessibility to the aqueous milieu (ΠNi) provide a powerful evaluation of the overall structure of lipid-embedded Ci-VSD. Data shown in panels B snd C of Figure 6 unambiguously demonstrate not only that S1 has a transmembrane topology but also that the topology defines its membrane boundaries and reveals an α-helical secondary structure. Comparison of the Ci-VSD environmental data with the relevant region of KvAP demonstrates the structural equivalence of the two molecules. The data were in the same range, and their oscillation pattern almost overlapped, strongly suggesting that in POPC/POPG liposomes Ci-VSD conforms to a scaffold common to that of known VSDs.

In summary, we have established a reliable prokaryotic expression system and biochemical preparation methods for the voltage-sensing domain of eukaryotic Ci-VSP. The protein is well-folded into the same scaffold as existing VSDs in a variety of detergents and lipid compositions. The interplay between functional and structural information from Ci-VSD should allow us to gain insights into the basic underpinnings of voltage sensor function. Furthermore, Ci-VSD's sequence is closer to that of the proton channel than all four available VSDs with successful biochemical preparations, and its structural information could provide a viable homology model for the proton channel.[4,5]

AUTHOR INFORMATION

Corresponding Author

*E-mail: eperozo@uchicago.edu. Phone: (773) 834-4747. Fax: (773) 834-4742.

Present Addresses

[†]D. E. Shaw Research, Hyderabad 500034, India.

[‡]Department of Cell Physiology, Health Sciences Center, Texas Tech University, Lubbock, TX 79430.

Funding

This work was supported in part by National Institutes of Health Grants R01-GM057846 and U54-GM087519 to E.P.

Notes

The authors declare no competing financial interest.

ACKNOWLEDGMENTS

We thank Francisco Benzanilla for kindly providing the cDNA of Ci-VSP in the Sp6 vector and allowing us unfettered access to the PTI fluorimeter. We thank Sudha Chakrapani and Jose Santos for providing comments and experimental advice in the early phases of this work.

ABBREVIATIONS

C_8E_4, *n*-octyltetraoxyethylene; Ci-VSD, voltage sensor domain of Ci-VSP; Ci-VSP, *C. intestinalis* voltage sensor-containing phosphatase; CW-EPR, continuous wave electron paramagnetic resonance; ΔH_o^{-1}, mobility as the inverse of the central line width of CW-EPR spectra; DDM, dodecyl D-maltoside; DM, decyl D-maltoside; FC-10, *n*-decylphosphocholine; GST, glutathione *S*-transferase; LDAO, lauryldimethylamine oxide; IPTG, isopropyl β-D-thiogalactopyranoside; MEGA-9, nonanoyl-*N*-methylglucamide; Ni-EDDA, nickel(II) ethylenediaminedi(*o*-hydroxyphenylacetic acid); OG, octyl D-glucoside; ΠNi, Ni-EDDA accessibility; ΠO_2, oxygen accessibility; POPC, 1-palmitoyl-2-oleoyl-*sn*-glycero-3-phosphocholine; POPE, 1-palmitoyl-2-oleoyl-*sn*-glycero-3-phosphoethanolamine; POPG, 1-palmitoyl-2-oleoyl-*sn*-glycero-3-[phospho-*rac*-(1-glycerol)]; SEC, size exclusion chromatography; VSD, voltage-sensing domain.

REFERENCES

(1) Bezanilla, F. (2008) How membrane proteins sense voltage. *Nat. Rev. Mol. Cell Biol. 9*, 323−332.

(2) Swartz, K. J. (2008) Sensing voltage across lipid membranes. *Nature 456*, 891−897.

(3) Murata, Y., Iwasaki, H., Sasaki, M., Inaba, K., and Okamura, Y. (2005) Phosphoinositide phosphatase activity coupled to an intrinsic voltage sensor. *Nature 435*, 1239−1243.

(4) Sasaki, M., Takagi, M., and Okamura, Y. (2006) A voltage sensor-domain protein is a voltage-gated proton channel. *Science 312*, 589−592.

(5) Ramsey, I. S., Moran, M. M., Chong, J. A., and Clapham, D. E. (2006) A voltage-gated proton-selective channel lacking the pore domain. *Nature 440*, 1213−1216.

(6) Bezanilla, F. (2000) The voltage sensor in voltage-dependent ion channels. *Physiol. Rev. 80*, 555−592.

(7) Noda, M., Shimizu, S., Tanabe, T., Takai, T., Kayano, T., Ikeda, T., Takahashi, H., Nakayama, H., Kanaoka, Y., Minamino, N., et al. (1984) Primary structure of *Electrophorus electricus* sodium channel deduced from cDNA sequence. *Nature 312*, 121−127.

(8) Armstrong, C. M., and Bezanilla, F. (1973) Currents related to movement of the gating particles of the sodium channels. *Nature 242*, 459−461.

(9) Mannuzzu, L. M., Moronne, M. M., and Isacoff, E. Y. (1996) Direct physical measure of conformational rearrangement underlying potassium channel gating. *Science 271*, 213−216.

(10) Tempel, B. L., Papazian, D. M., Schwarz, T. L., Jan, Y. N., and Jan, L. Y. (1987) Sequence of a probable potassium channel component encoded at Shaker locus of *Drosophila*. *Science 237*, 770−775.

(11) Bezanilla, F., and Stefani, E. (1998) Gating currents. *Methods Enzymol. 293*, 331−352.

(12) Schwarz, T. L., Tempel, B. L., Papazian, D. M., Jan, Y. N., and Jan, L. Y. (1988) Multiple potassium-channel components are produced by alternative splicing at the Shaker locus in *Drosophila*. *Nature 331*, 137−142.

(13) Villalba-Galea, C. A., Sandtner, W., Starace, D. M., and Bezanilla, F. (2008) S4-based voltage sensors have three major conformations. *Proc. Natl. Acad. Sci. U.S.A. 105*, 17600−17607.

(14) Jiang, Y., Lee, A., Chen, J., Ruta, V., Cadene, M., Chait, B. T., and MacKinnon, R. (2003) X-ray structure of a voltage-dependent K^+ channel. *Nature 423*, 33−41.

(15) Butterwick, J. A., and MacKinnon, R. (2010) Solution structure and phospholipid interactions of the isolated voltage-sensor domain from KvAP. *J. Mol. Biol. 403*, 591−606.

(16) Long, S. B., Tao, X., Campbell, E. B., and MacKinnon, R. (2007) Atomic structure of a voltage-dependent K^+ channel in a lipid membrane-like environment. *Nature 450*, 376−382.

(17) Payandeh, J., Scheuer, T., Zheng, N., and Catterall, W. A. (2011) The crystal structure of a voltage-gated sodium channel. *Nature 475*, 353−358.
(18) Zhang, X., Ren, W., DeCaen, P., Yan, C., Tao, X., Tang, L., Wang, J., Hasegawa, K., Kumasaka, T., He, J., Clapham, D. E., and Yan, N. (2012) Crystal structure of an orthologue of the NaChBac voltage-gated sodium channel. *Nature 486*, 130−134.
(19) Tombola, F., Pathak, M. M., Gorostiza, P., and Isacoff, E. Y. (2007) The twisted ion-permeation pathway of a resting voltage-sensing domain. *Nature 445*, 546−549.
(20) Starace, D. M., and Bezanilla, F. (2004) A proton pore in a potassium channel voltage sensor reveals a focused electric field. *Nature 427*, 548−553.
(21) Sutton, K. A., Jungnickel, M. K., Jovine, L., and Florman, H. M. (2012) Evolution of the Voltage Sensor Domain of the Voltage-Sensitive Phosphoinositide Phosphatase, VSP/TPTE, Suggests a Role as a Proton Channel in Eutherian Mammals. *Mol. Biol. Evol. 29*, 2147−2155.
(22) Li, Q., and Fung, L. W. (2009) Structural and dynamic study of the tetramerization region of non-erythroid α-spectrin: A frayed helix revealed by site-directed spin labeling electron paramagnetic resonance. *Biochemistry 48*, 206−215.
(23) Chakrapani, S., Cuello, L. G., Cortes, D. M., and Perozo, E. (2008) Structural dynamics of an isolated voltage-sensor domain in a lipid bilayer. *Structure 16*, 398−409.
(24) Vasquez, V., Cortes, D. M., Furukawa, H., and Perozo, E. (2007) An optimized purification and reconstitution method for the MscS channel: Strategies for spectroscopical analysis. *Biochemistry 46*, 6766−6773.
(25) Cuello, L. G., Cortes, D. M., and Perozo, E. (2004) Molecular architecture of the KvAP voltage-dependent K^+ channel in a lipid bilayer. *Science 306*, 491−495.
(26) Cuello, L. G., Romero, J. G., Cortes, D. M., and Perozo, E. (1998) pH-dependent gating in the *Streptomyces lividans* K^+ channel. *Biochemistry 37*, 3229−3236.
(27) Perozo, E., Cortes, D. M., and Cuello, L. G. (1998) Three-dimensional architecture and gating mechanism of a K^+ channel studied by EPR spectroscopy. *Nat. Struct. Biol. 5*, 459−469.
(28) Cortes, D. M., and Perozo, E. (1997) Structural dynamics of the *Streptomyces lividans* K^+ channel (SKC1): Oligomeric stoichiometry and stability. *Biochemistry 36*, 10343−10352.
(29) Killian, J. A. (1998) Hydrophobic mismatch between proteins and lipids in membranes. *Biochim. Biophys. Acta 1376*, 401−415.
(30) Lee, S. Y., Lee, A., Chen, J., and MacKinnon, R. (2005) Structure of the KvAP voltage-dependent K^+ channel and its dependence on the lipid membrane. *Proc. Natl. Acad. Sci. U.S.A. 102*, 15441−15446.
(31) Milescu, M., Bosmans, F., Lee, S., Alabi, A. A., Kim, J. I., and Swartz, K. J. (2009) Interactions between lipids and voltage sensor paddles detected with tarantula toxins. *Nat. Struct. Mol. Biol. 16*, 1080−1085.
(32) Schmidt, D., Jiang, Q. X., and MacKinnon, R. (2006) Phospholipids and the origin of cationic gating charges in voltage sensors. *Nature 444*, 775−779.
(33) Kohout, S. C., Ulbrich, M. H., Bell, S. C., and Isacoff, E. Y. (2008) Subunit organization and functional transitions in Ci-VSP. *Nat. Struct. Mol. Biol. 15*, 106−108.
(34) Chakrapani, S., Sompornpisut, P., Intharathep, P., Roux, B., and Perozo, E. (2010) The activated state of a sodium channel voltage sensor in a membrane environment. *Proc. Natl. Acad. Sci. U.S.A. 107*, 5435−5440.
(35) Vistnes, A. I., and Puskin, J. S. (1981) A spin label method for measuring internal volumes in liposomes or cells, applied to Ca-dependent fusion of negatively charged vesicles. *Biochim. Biophys. Acta 644*, 244−250.
(36) Chanda, B., Asamoah, O. K., Blunck, R., Roux, B., and Bezanilla, F. (2005) Gating charge displacement in voltage-gated ion channels involves limited transmembrane movement. *Nature 436*, 852−856.
(37) Jiang, Y., Ruta, V., Chen, J., Lee, A., and MacKinnon, R. (2003) The principle of gating charge movement in a voltage-dependent K^+ channel. *Nature 423*, 42−48.
(38) Xu, Y., Ramu, Y., and Lu, Z. (2010) A Shaker K^+ channel with a miniature engineered voltage sensor. *Cell 142*, 580−589.

NOTE ADDED AFTER ASAP PUBLICATION

This manuscript was published ASAP on October 5, 2012. Corrections were made to Table 1 and the revised version was reposted on October 16, 2012.